Structure, phase transitions and molecular motions in 4-aminopyridinium perchlorate

2002 J. Phys.: Condens. Matter 14 8497

(http://iopscience.iop.org/0953-8984/14/36/308)

INSTITUTE OF PHYSICS PUBLISHING JOURNAL OF PHYSICS: CONDENSED MATTER

J. Phys.: Condens. Matter **14** (2002) 8497–8512 PII: S0953-8984(02)36279-9

Structure, phase transitions and molecular motions in 4-aminopyridinium perchlorate

O Czupiński[1], G Bator[1], Z Ciunik[1], R Jakubas[1,3], W Medycki[2] and J Świergiel[2,4]

[1] Faculty of Chemistry, University of Wrocław, Joliot-Curie 14, 50-383 Wrocław, Poland
[2] Institute of Molecular Physics, PAS, Smoluchowskiego 17, 60-179 Poznań, Poland

Received 26 April 2002
Published 29 August 2002
Online at stacks.iop.org/JPhysCM/14/8497

Abstract

The crystal structure of the 4-aminopyridinium perchlorate (4-apyH)ClO_4 has been determined at 100 K by means of x-ray diffraction as monoclinic, with space group $P2_1$, with $Z = 8$. The crystal undergoes two structural phase transitions: one of first-order type, reversible, at 241/243 K (on cooling/heating respectively) and one of weakly first-order type, irreversible, at 277 K (on heating). The crystal dynamics is discussed on the basis of the temperature dependence of the ^{1}H nuclear magnetic resonance second moment (M_2) and spin–lattice relaxation time T_1. Both phase transitions are interpreted in terms of the changes in the motional state of $(4\text{-apyH})^+$ cations and ClO_4^- anions. The dielectric dispersion studies disclose a relaxation process over the high-temperature phase (above 241 K) in the audio-frequency region. The dielectric results are described by a Cole–Cole equation. The title crystal reveals pyroelectric properties below 241 K. The ferroelastic domain structure of (4-apyH)ClO_4 is observed over the whole temperature range studied.

1. Introduction

Recently, much attention has been devoted to simple molecular–ionic crystals containing organic cations and acid radicals (1:1 molar ratio) due to the tunability of their special structural features and their interesting physical properties. The heteroaromatic pyridine cations with BF_4^-, ClO_4^-, ReO_4^- and IO_4^- anions constitute a large group of such materials exhibiting ferroelectric properties [1–4]. Very recently, mono-salts of 1, 4-diazobicyclo[2.2.2]octane, $(C_6H_{13}N_2)ClO_4$ and $(C_6H_{13}N_2)BF_4$, were found to show ferroelectricity at room temperature [5]. The most intriguing feature of these crystals is the fact that the polar properties are determined by the disordering of the protons in the $N–H^+\cdots N$ hydrogen bonds forming linear chains. In the search for new polar materials it seemed to be of interest to incorporate into

[3] Author to whom any correspondence should be addressed.
[4] On leave of an absence from: The Institute of Physics, A Mickiewicz University, Poznań, Poland.

the crystal lattices of such simple salts substituted pyridinium cation such as 4-aminopyridinium ones. Since it is bestowed on a specific dipole moment, the change in the dynamical state of such cations should be reflected in the dielectric properties of the crystals.

Crystal structure and IR spectroscopic studies of 4-aminopyridine hemiperchlorate (4-apy)$\cdot\frac{1}{2}HClO_4$ have already been reported [6, 7]. It contains asymmetrical H-bridged $(4\text{-apy}\cdots H\cdots 4\text{-apy})^+$ cations. This crystal exhibits a polymorphism, but it has turned out that the two different phases (α and β) belong to the same space group ($P2_1/c$). We have succeeded in obtaining a new 4-aminopyridinium analogue, namely (4-apyH)ClO_4.

In this paper we present x-ray, calorimetric, dilatometric, dielectric dispersion and proton magnetic resonance (^{1}H NMR) studies of the (4-apyH)ClO_4 crystal. A mechanism is proposed for the phase transitions in the title crystal.

2. Experimental details

(4-apyH)ClO_4 was prepared by treating concentrated perchlorate acid with an aqueous solution of 4-aminopyridine. The colourless crystalline product was filtered off and washed and then recrystallized from acetonitrile. Single crystals of (4-apyH)ClO_4 were obtained by slow evaporation of the acetonitrile solution at room temperature. The chemical formula of the compound was checked by elemental analysis (found: C, 30.74; H, 3.78; N, 14.74%; calculate: C, 30.93; H, 3.64; N, 14.44%).

The complex electric permittivity $\varepsilon^* = \varepsilon' - i\varepsilon''$ in the temperature range from 200 to 300 K was measured with HP 4284 A and HP 4285 A Precision LCR Meters over a frequency range between 1 kHz and 20 MHz and with an HP 4191 A impedance analyser over the frequency range between 30 and 900 MHz. The dimensions of the sample were of the order of $3 \times 3 \times 1$ mm^3. The overall error was less than 5 and 10% for the real and imaginary part of the complex electric permittivity, respectively.

Differential scanning calorimetry (DSC) was recorded using a Perkin-Elmer DSC-7 over the temperature range 100–400 K.

The dilatometric measurements were made with a thermomechanical analyser, Perkin-Elmer TMA-7, over the temperature range 200–300 K. The dimensions of the sample were of the order of $3 \times 3 \times 1$ mm^3.

The pyroelectric charge was measured by a Keithley 617 electrometer.

The experiments measuring the spin–lattice relaxation of the Zeeman system and the second moment M_2 were made on a SXP 4/100 Bruker pulse spectrometer at 90 MHz for protons. Proton relaxation times T_1 were measured employing a π–τ–$\pi/2$ pulse sequence for times shorter than 1 s and by a conventional saturation–recovery technique with a saturation sequence of fifteen 90° pulses, each followed by a 4 ms delay, for times longer than 1 s. The second moment of the ^{1}H NMR line was found from the analysis of the shape dependence of a 'solid echo'. The temperature of the specimen was automatically kept constant by a Bruker BS 100/700 temperature controller.

3. Results

3.1. Crystal structure description

Data for the structure determination were collected using an Oxford Cryosystem device on a Kuma KM4CCD κ-axis diffractometer with graphite-monochromated Mo Kα radiation at 293 and 100 K. The crystal was positioned at 65 mm from the CCD camera. 612 frames were measured at 0.75° intervals with a counting time of 15 s. Accurate cell parameters were determined and refined by least-squares fitting of angular data on 1200 (293 K) and 3500

Table 1. Parameters of data collection and structure refinement for (4-apyH)ClO_4. (Note: crystallographic data for the structures reported in this paper (excluding structure factors) have been deposited with the Cambridge Crystallographic Data Centre, CCDC No 167865. Copies of this information may be obtained free of charge from the Director, CCDC, 12 Union Road, Cambridge CB2 1EZ, UK (fax: +44-1223-336033; e-mail: deposit@ccdc.cam.ac.uk or http://www.ccdc.cam.ac.uk).)

Empirical formula	$C_5H_7ClN_2O_4$
Formula weight	194.58
Temperature (K)	100(2)
Crystal system	Monoclinic
Space group	$P2_1$
a (Å)	10.737(2)
b (Å)	8.9500(18)
c (Å)	16.677(3)
β (deg)	107.28(3)
Volume (Å^3)	1530.3(5)
Z	8
μ (Mo Kα) (mm^{-1})	0.475
$F(000)$	800
θ-range (deg)	3.42–28.39
Index ranges	$-13 \leqslant h \leqslant 11$, $-11 \leqslant k \leqslant 11$, $-19 \leqslant l \leqslant 22$
Reflections collected	10 572
Goodness-of-fit (F^2)	1.077
Final R_1/wR_2 indices ($I > 2\sigma_I$)	0.0603/0.1891

(100 K) of the strongest reflections. The data were corrected for Lorentz and polarization effects. No absorption correction was applied. Data collection and integration and scaling of the reflections were achieved using the CrysAlis suite of programs [8]. Space groups were determined on all reflections collected at fixed temperatures using the XPREP program [9]. Crystallographic data obtained at room and low temperature showed the existence of phase transitions between room temperature and 100 K, in which the structure changes from one monoclinic lattice to another. The data collected suggest the $C2$ space group with lattice parameters $a = 7.768(3)$, $b = 9.052(3)$, $c = 5.964(2)$ Å, $\beta = 103.71(2)^\circ$ and $V = 407.4(2)$ Å^3 at room temperature and the $P2_1$ space group at 100 K. The data collection parameters and the structural refinement results for the latter phase are listed in table 1. Moreover, at 100 K, coexistence of two identical monoclinic lattices with the space group $P2_1$ in the crystal studied was observed. The dominant lattice was indicated by about 80% of the indexed reflections and the minor one by about 15% of the reflections. The angle between the $\boldsymbol{c}^*$-vectors of the respective reciprocal lattices (the angle between $\boldsymbol{c}_1^*$ and $\boldsymbol{c}_2^*$) was about 26° whereas the angles between $\boldsymbol{a}_1^*$ and $\boldsymbol{a}_2^*$ and between $\boldsymbol{b}_1^*$ and $\boldsymbol{b}_2^*$ were equal about 120°. This result and our other optical observations with the polarized light suggest that the crystals studied have a domain structure.

Single-crystal analysis of data collected at 293 K (4266 measured and 783 unique reflections; $R_{int} = 0.038$) showed that all molecules are fully disordered and structure parameters cannot be precisely determined. In the next step, reflections which satisfied diffraction conditions in the minor lattice at low temperature were excluded from the crystal structure determination. The low-temperature structure was solved by direct methods (program SHELXS97 [10]) and refined by the full-matrix least-squares method on all F^2-data using the SHELXL97 [11] programs. Non-hydrogen atoms were refined with anisotropic displacement parameters; hydrogen atoms were included from the geometry of molecules and $\Delta\rho$ maps but were not refined.

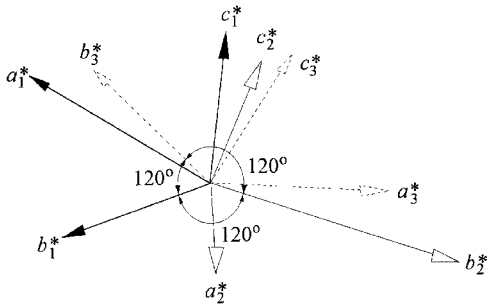

Figure 1. The spatial arrangement of reciprocal lattices of the observed domains in the crystal at 100 K.

For confirmation of the spatial arrangement of domains at low temperature in the crystals studied, another large and recently recrystallized specimen with readily recognizable domain structure at room temperature was selected. The crystal was slowly cooled at a constant rate of 60 K h^{-1} down to 100 K and measurements were made on a Kuma KM4CCD diffractometer by the method presented above with a counting time of 5 s. 3688 of the strongest reflections were used for lattice parameter determination. 1811 reflections (49.1%) indicated the first domain, 948 (25.7%) and 874 (23.8%) indicated the other two domains. Figure 1 shows the spatial arrangement of the reciprocal lattices of the observed domains in the crystal at 100 K. All angles between respective vectors (between $\boldsymbol{a}_i^*$ and $\boldsymbol{a}_j^*$; $\boldsymbol{b}_i^*$ and $\boldsymbol{b}_j^*$; $\boldsymbol{c}_i^*$ and $\boldsymbol{c}_j^*$; where $i, j = 1$, 2 and 3) are similar to those in the first crystal. The spatial arrangement of the domain axes is similar to that observed in the first crystal. It suggests a trigonal lattice as a prototype symmetry of the crystals studied.

The crystal structure of the title compound consists of discrete ClO_4^- anions and $(4\text{-apyH})^+$ cations which are bonded to each other by N–H $\cdots$ O hydrogen bonds. Selected bond lengths and angles and hydrogen contacts are given in table 2. At 100 K both anions and organic cations are ordered. The numbering scheme is shown in figure 2(a). There are four symmetry-independent ClO_4^- anions and four 4-aminopyridinium cations. The packing of the crystal structure is illustrated in figure 2(b). All pyridinium rings are placed in the plane, which is perpendicular to the [001] direction. In the N–H $\cdots$ O hydrogen bond system, both the NH_2 groups and protonated N atoms of the ring are involved. Two pairs of 4-aminopyridinium cations (N(1) and N(2) or N(3) and N(4)) are situated antiparallel to each other. On the other hand, if we compare the C–NH_2 bond lengths for the cations we see clearly that these distances are quite different; e.g. for C(13)–N(12) and C(23)–N(22) they are equal to 1.338(4) and 1.270(4) Å, respectively, and for C(33)–N(32) and C(43)–N(42) they are 1.339(4) and 1.323(5) Å, respectively. Such a system strongly stabilizes the anionic and cationic sublattices. In the low-temperature phase, for the well-ordered tetrahedral perchlorate anions, the Cl–O distances range from 1.393(3) to 1.470(3) Å (for the most distorted tetrahedron: from 1.393(4) to 1.436(3) Å), whereas the angles are in the range from 107.72° to 111.0°, which agrees well with the corresponding values found for other perchlorates [6, 7]. Distances and angles within the 4-aminopyridinium cations are normal [12].

The amino groups deviated insignificantly from the ring plane: N(42): 0.054(5); N(32): 0.003(5); N(22): 0.022(5); N(12): 0.018(5) Å. There is no correlation of this deviation with the length of the C–NH_2 bond. The NH_2 groups for all types of cation are bonded to the O atoms by shorter hydrogen bonds (from 2.964 to 3.120 Å) in comparison to those formed by protonated N atoms. It should be added that the hydrogen bonds formed by the latter atoms

Table 2. Selected bond lengths (Å) and bond angles (deg) and hydrogen bond distances and angles for (4-apyH)ClO_4. Footnotes: symmetry transformations used to generate equivalent atoms.

Anion		Anion	
	Bond length (Å)	Bond angle (deg)	Bond angle (deg)
Cl(1)–O(13)	1.436(3)	O(13)–Cl(1)–O(11)	110.9(2)
Cl(1)–O(11)	1.442(3)	O(13)–Cl(1)–O(12)	109.66(16)
Cl(1)–O(12)	1.448(2)	O(11)–Cl(1)–O(12)	109.97(19)
Cl(1)–O(14)	1.470(3)	O(13)–Cl(1)–O(14)	108.30(18)
Cl(2)–O(21)	1.435(3)	O(11)–Cl(1)–O(14)	108.83(19)
Cl(2)–O(22)	1.437(3)	O(12)–Cl(1)–O(14)	109.18(15)
Cl(2)–O(24)	1.440(2)	O(21)–Cl(2)–O(22)	110.35(17)
Cl(2)–O(23)	1.450(3)	O(21)–Cl(2)–O(24)	110.61(16)
Cl(3)–O(32)	1.411(3)	O(22)–Cl(2)–O(24)	109.02(15)
Cl(3)–O(31)	1.444(2)	O(21)–Cl(2)–O(23)	109.65(16)
Cl(3)–O(34)	1.451(3)	O(22)–Cl(2)–O(23)	107.72(16)
Cl(3)–O(33)	1.451(3)	O(24)–Cl(2)–O(23)	109.44(15)
Cl(4)–O(41)	1.393(4)	O(32)–Cl(3)–O(31)	110.12(18)
Cl(4)–O(42)	1.410(3)	O(32)–Cl(3)–O(34)	110.87(18)
Cl(4)–O(44)	1.429(3)	O(31)–Cl(3)–O(34)	108.22(15)
Cl(4)–O(43)	1.446(3)	O(32)–Cl(3)–O(33)	110.21(19)
		O(31)–Cl(3)–O(33)	108.23(16)
Cation		O(34)–Cl(3)–O(33)	109.13(16)
		O(41)–Cl(4)–O(42)	111.0(2)
	Bond length (Å)	O(41)–Cl(4)–O(44)	108.4(2)
		O(42)–Cl(4)–O(44)	109.76(17)
N(12)–C(13)	1.338(4)	O(41)–Cl(4)–O(43)	108.3(2)
N(22)–C(23)	1.270(4)	O(42)–Cl(4)–O(43)	109.05(17)
N(32)–C(33)	1.399(4)	O(44)–Cl(4)–O(43)	110.26(17)
N(42)–C(43)	1.323(5)		

Hydrogen contacts	Bond length (Å)		Bond angle (deg)
D–H···A	d(H···A)	d(D···A)	<(DHA)
N(21)–H(21)···O(34)[a]	2.31	3.053(4)	142.6
N(31)–H(31)···O(42)[b]	2.22	2.971(4)	142.6
N(41)–H(41)···O(42)[d]	2.27	3.018(4)	142.9
N(32)–H(132)···O(43)[d]	2.02	3.084(4)	165.2
N(42)–H(142)···O(22)[c]	2.15	3.020(4)	168.0
N(12)–H(112)···O(33)[e]	2.02	2.964(4)	169.6
N(22)–H(122)···O(13)	2.11	3.120(4)	165.1
N(22)–H(222)···O(44)	2.40	3.335(5)	156.0
N(32)–H(232)···O(12)[d]	2.43	3.343(5)	161.9

[a] $-x+2, y-1/2, -z+1$ [b] $x-1, y-1, z$ [c] $x-1, y, z$
[d] $x, y-1, z$ [e] $-x+2, y+1/2, -z+1$.

are usually strongly non-linear. One can state that the present hydrogen bond configuration in (4-apyH)ClO_4 at 100 K reflects the full ordering of the anionic and cationic units.

3.2. Thermal behaviour of (4-apyH)ClO_4

In order to detect structural phase transitions in (4-apyH)ClO_4, DSC and dilatometric measurements have been undertaken. The DSC curves obtained for (4-apyH)ClO_4 crystals during cooling and heating scans are presented in figure 3(a). The calorimetric measurements

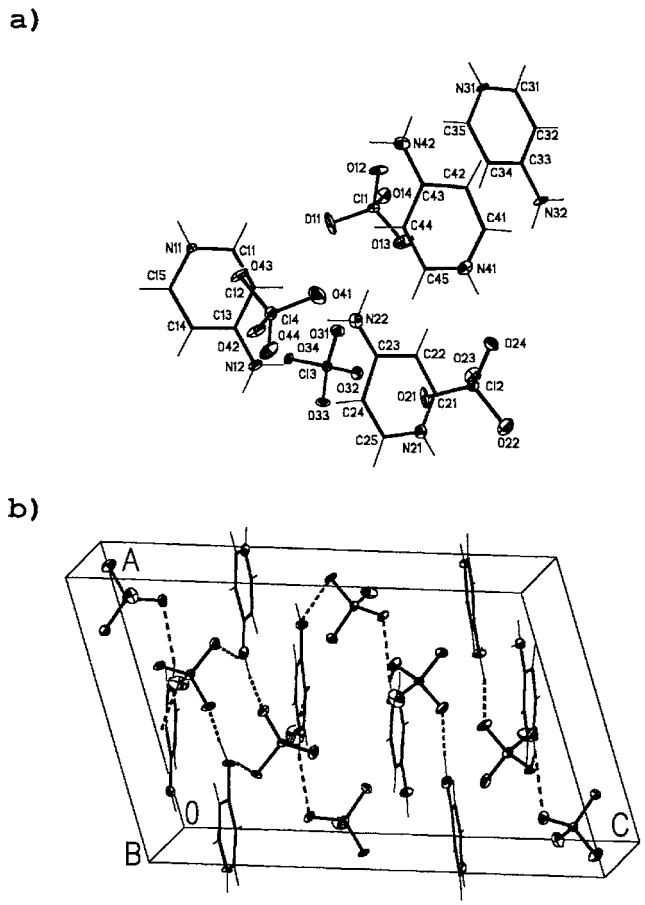

Figure 2. (a) Independent parts of the unit cell of (4-apyH)ClO_4 at 100 K with the atom labelling scheme. The ellipsoids for N, Cl and O atoms are drawn at 50% probability. (b) The unit cell of (4-apyH)ClO_4 viewed along the *b*-axis.

show that we are dealing with reversible phase transitions of first-order type at 241/243 K on cooling/heating runs. The temperature hysteresis extrapolated to zero scanning rate is equal to 2 K. The transition entropy value $\Delta S = 17 \pm 2$ J mol^{-1} K^{-1} indicates an 'order–disorder' phase transition.

It should be added that at $T = 277$ K another small anomaly has been found on the heating scan. This is not, however, observed on cooling. This anomaly is suggested to be related to a weakly first-order (or continuous) phase transition. The nature of the phase transition at 277 K is rather sophisticated. A small value of the entropy change may suggest that this transition is of the 'displacive' type. The lack of a DSC anomaly on cooling might be connected with a small value of the heat effect but not with irreversibility of the transition.

Figure 3(b) shows results on the linear thermal expansion, $\Delta L/L_0$, measured along the *b*-axis (the directions presented correspond to those taken for the low-temperature monoclinic phase). Step-wise changes in dimensions of the crystal are clearly seen at 241/243 K on cooling/heating, respectively. In the two analysis directions, *b* and *c* (not shown), the

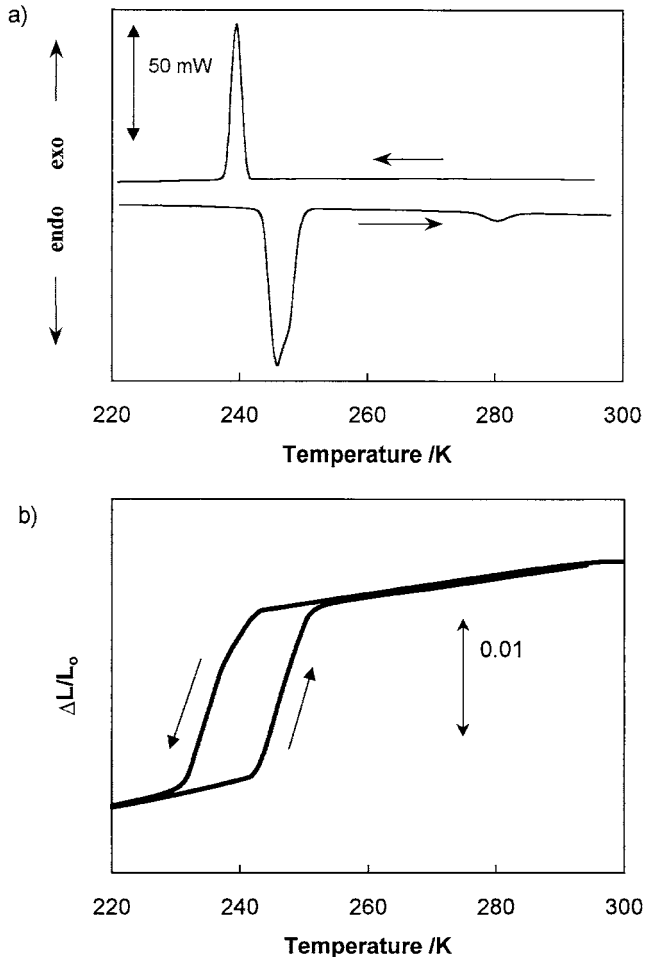

Figure 3. (a) DSC curves for the (4-apyH)ClO_4 crystals for the cooling and heating runs (10 K min^{-1}, $m = 25.82$ mg). (b) Temperature dependences of the linear thermal expansion for samples along the b-axis (monoclinic symmetry, $P2_1$) during cooling and heating runs.

dimension of the crystal diminishes on cooling, with comparable values of $\Delta L/L_0$ equal to about 0.015, and is perfectly reversible with temperature. It was impossible to estimate the change in the volume of the crystal, $\Delta V/V$, at the 241 K phase transition, since we did not succeed in obtaining a well-shaped single crystal along the a-axis. Most probably the crystal volume diminishes after the transition to the low-temperature phase. The presence of distinct temperature hysteresis in the $\Delta L/L_0$ versus temperature curves is related to the fact that we are dealing with a first-order phase transition. The average temperature coefficients of the linear thermal expansion, $\bar{\alpha} = \Delta L/(L_0\,\Delta T)$, in the b-direction are positive, both below and above the phase transition point. The values of $\bar{\alpha}_b$ in the high-and low-temperature phases are of the order of 4×10^{-4} and 5×10^{-4} K^{-1}, respectively. For the c-direction the $\bar{\alpha}$-coefficients are comparable. We should add that in the vicinity of the postulated phase transition at 277 K, no anomaly in the dilation is observed.

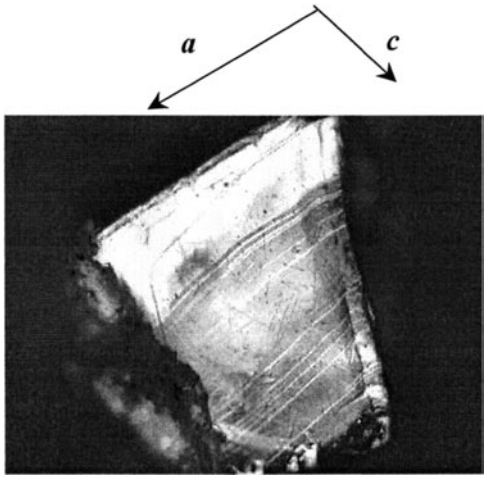

Figure 4. Ferroelastic domain structure in the a–c plane of (4-apyH)ClO_4 at 300 K.

3.3. Optical observations

As-grown single crystals of (4-apyH)ClO_4 are usually monodomain. If a small mechanical stress is applied along the a- or c-direction the crystal will show ferroelastic domains in the a–c plane at room temperature (see figure 4). We were able to observe only one type of domain wall parallel to that of the edge of a pseudo-hexagonal plate of the sample (a–c plane). Since this material has the feature of being a very soft plastic crystal, each external mechanical stress necessary to induce the ferroelastic domains deforms the single crystal considerably. That is why the visible domains walls are slightly corrugated. On cooling, when the 241 K phase transition takes place the domain walls do not change; however, the presence of a clear phase front corroborates the first-order character of this transition.

3.4. Dielectric properties

The purpose of these measurements was to determine the dynamics of the dipole groups in the vicinity of the structural phase transitions. The measurements of the complex electric permittivity, ε^*, of (4-apyH)ClO_4 as a function of temperature (200–300 K) and frequency (1 kHz–30 MHz) were performed along the b-axis during cooling. Figure 5 shows the temperature dependence of the real part of the complex electric permittivity, ε'_b, in the vicinity of the phase transition at 241/243 K (on cooling/heating) at frequency of 1 MHz. At the phase transition temperature, one can observe a discontinuous change in the ε'_b-value, which is perfectly reversible on heating. The observed dielectric increment, $\Delta\varepsilon_b$, is quite large, being of the order of 14 units, and it is independent of the applied frequency of the electric field. Such a $\varepsilon'_b(T)$ characteristic is typical of first-order phase transition, which is in agreement with the DSC and dilatometric results. The shape of the dielectric anomaly in the vicinity of the phase transition resembles those found for plastic crystals characterized by the free rotational motion of spherical dipolar groups. In this instance, dielectric dispersion and absorption should be observed if the frequency of the rotational motion is comparable to that of the measuring electric field. Since no dispersion or absorption is found in the frequency range between 1 and 30 MHz, it should be expected at frequencies higher than 30 MHz.

Figure 6 shows ε'_b versus temperature in the high-frequency range (between 30 and 900 MHz). It has been found that the dielectric response in the (4-apyH)ClO_4 crystals is

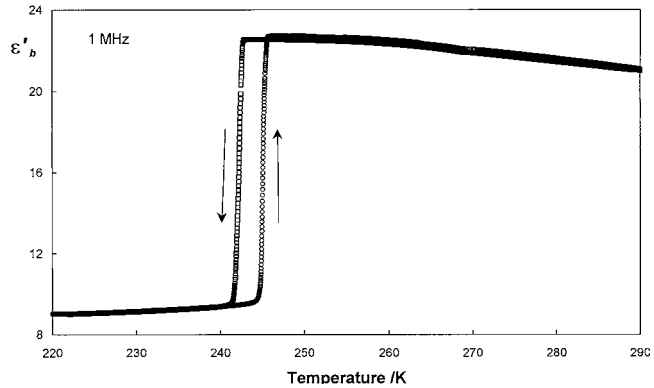

Figure 5. The temperature dependence of ε' for the (4-apyH)ClO_4 crystals along the *b*-axis.

well described by the empirical Cole–Cole relation [13]:

$$\varepsilon^* = \varepsilon_\infty + \frac{\varepsilon_0 - \varepsilon_\infty}{1 + (\mathrm{i}\omega\tau)^{1-\alpha}}, \tag{1}$$

where ε_0 and ε_∞ are the low-and high-frequency limits of the electric permittivity, respectively, ω is angular frequency, τ is the macroscopic relaxation time and α is a parameter of the distribution of relaxation times.

The Argand diagrams at selected temperatures (between 244 and 275 K) above the phase transition temperature $T_c = 241$ K are presented in figure 7. These dielectric results indicate a diffuse dielectric response with a possible distribution of relaxation times.

We have fitted the experimental Argand plots at several temperatures with equation (1) and determined the fitting parameters ε_0, ε_∞, τ and α. The energy barrier E_a was estimated from the Arrhenius relation for the relaxation time:

$$\tau = C \exp(E_a/RT). \tag{2}$$

The temperature dependence of the estimated relaxation time, τ, shows two temperature regions. Above the phase transition point (241 K) up to 260 K the macroscopic relaxation time, $\tau \approx 1.5 \times 10^{-10}$ s at T_c, depends very weakly on temperature, indicating that the activation energy is very small ($\sim$4 kJ mol^{-1}). A significant shortening of τ observed above 260 K is related either to an increase of activation energy in this temperature region or to differentiation of relaxators contributing to the dielectric response with increasing temperature. The value of E_a is usually burdened by a relatively large error; we can only state that above 260 K its roughly estimated value is of the order of 30 kJ mol^{-1}. It should be emphasized that the dielectric characteristics, both static and dynamic, are perfectly reversible in the vicinity of the 241 K phase transition.

3.5. Pyroelectric measurements

To throw more light on the polar properties of the phases both above (space group $C2$) and below 241 K (space group $P2_1$), pyroelectric measurements have been carried out. It should be emphasized that both phases are polar, but there is no simple relationship between the polar directions in the two phases. As a result it is impossible to determine the absolute values of P_s in corresponding phases; one can only determine the change in the projection of P_s on the measuring direction. The spontaneous polarization as a function of temperature is shown in figure 8. The measurements were performed in the *b*-direction corresponding to

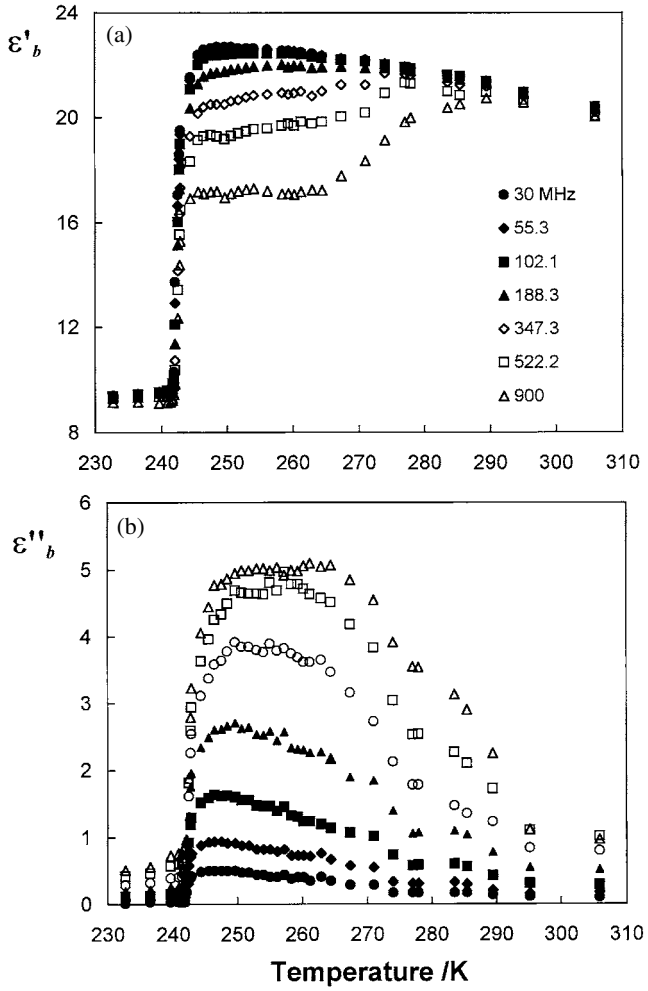

Figure 6. Temperature dependences of ε'_b (a) and of ε''_b (b) for the (4-apyH)ClO_4 crystal over the frequency range 30–900 MHz.

the low-temperature phase. The result confirms clearly the polar properties of the lowest-temperature phase. A relatively small change in the spontaneous polarization value, of the order of 3×10^{-6} C m^{-2}, appears below 243 K. Unfortunately, it is not reversed under the external dc electric field. It can be concluded, therefore, that (4-apyH)ClO_4 may be classified as a pyroelectric crystal below 243 K, which supports the crystallographic results.

3.6. ^1H *NMR studies*

The observed temperature dependence of the second moment, M_2, of the proton resonance lines for polycrystalline (4-apyH)ClO_4 salt is shown in figure 9(a). Over the lowest-temperature phase between 174 and 243 K, the second moment possesses a plateau of about 5.5×10^{-8} T^2. Between 243 and 277 K, M_2 monotonically decreases, approaching a value of 2.8×10^{-8} T^2. Over the high-temperature phase up to 300 K, the M_2-value again shows a plateau of 2.6×10^{-8} T^2.

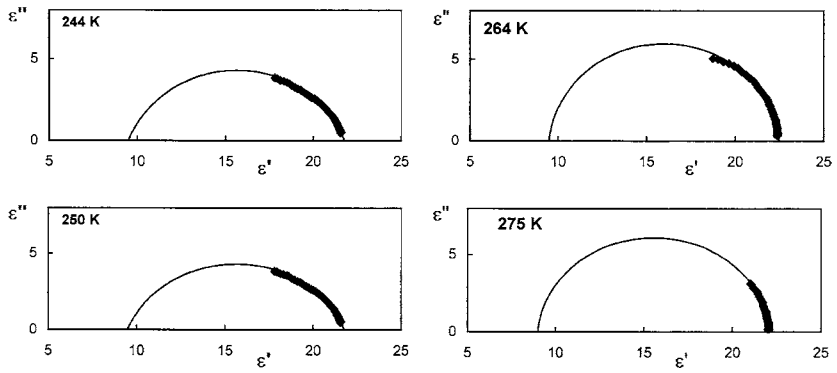

Figure 7. Argand diagrams for the (4-apyH)ClO_4 crystals over the high-temperature phase.

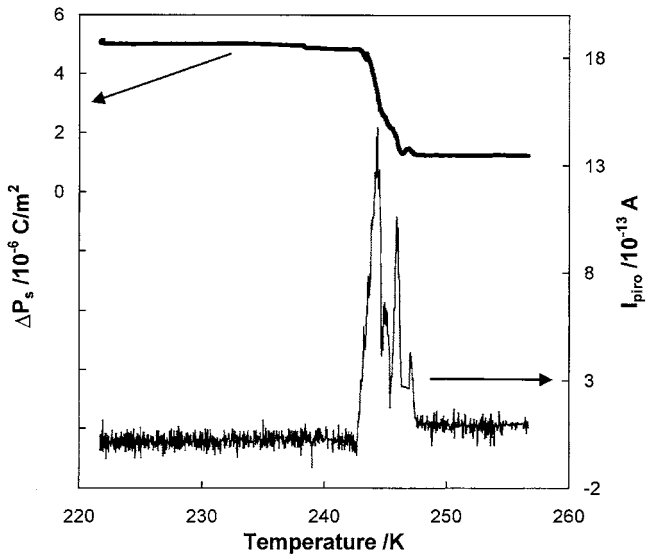

Figure 8. The temperature dependence of the spontaneous polarization change, ΔP_s, and pyroelectric current, I_{piro}, for the (4-apyH)ClO_4 crystal in the vicinity of the 243 K phase transition (on heating).

The theoretical second-moment value was calculated using van Vleck's formula [14] for five possible motional states of the 4-apyH cation: (1) a rigid cation; (2) reorientation of a rigid cation about the C_2 axis; (3) a cation performing reorientation about a pseudo-sixfold axis perpendicular to the pyridinium ring—C_6'; (4) reorientation of the NH_2 group with a rigid pyridinium ring; and (5) reorientation of NH_2 with the C_6' motion (table 3). The highest M_2-value observed (5.5×10^{-8} T^2 at 174 K) is lower than the intracationic part of the second moment calculated for the rigid cations, even without the intercationic part. This may suggest that three of four non-equivalent cations are disordered at this temperature in such a way that the NH_2 groups are performing reorientations and the pyridinium rings are rigid. The fourth cation is rigid as a whole. The theoretical total value of M_2 obtained for such a model is equal to 5.5×10^{-8} T^2 (containing the intercationic part equal to 1.3×10^{-8} T^2), which is close to the observed value of M_2.

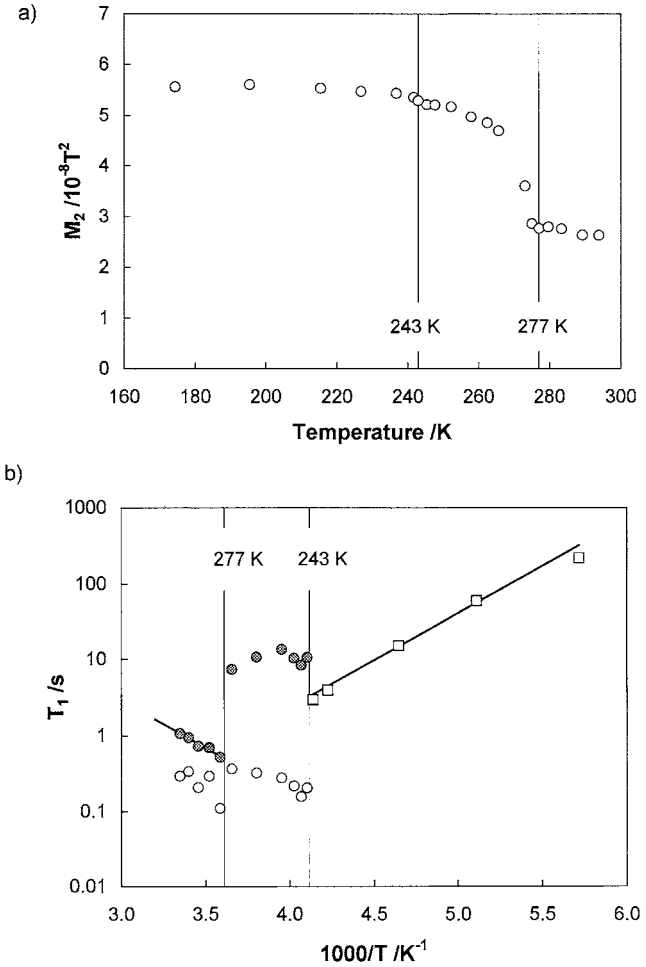

Figure 9. (a) The temperature dependence of the second moment of the proton NMR lines for (4-apyH)ClO_4; (b) spin–lattice relaxation times, T_1, versus $1000/T$ at 90 MHz. For the temperature range above 243 K: open circles: short-time component, T_1^S; full circles: long-time component, T_1^L.

Table 3. Calculated second-moment values (M_2) of the (4-apyH$^+$) cation.

Model of reorientation	Intramolecular part of second moment of ^{1}H NMR line (10^{-8} T^2)
Rigid cation	6.67
Reorientation of a rigid cation about C_2	2.02
Reorientation of a rigid cation about pseudo-sixfold axis (C_6')	0.81
Reorientation of NH_2 with rigid pyridinium ring	3.42
Reorientation of NH_2 + the C_6' reorientation	0.17

Approaching the phase transition point, 277 K, from below, one can observe continuous diminishing of the second-moment value which may be explained in terms of the onset of

reorientations of all 4-apyH cations. The plateau observed above 277 K cannot be attributed to just one type of reorientation mode of the 4-apyH cation. Hashimoto *et al* [15] proposed, for crystal containing the same organic cation, –(4-apyH)$SbBr_4$, only the reorientations around a pseudo-sixfold axis of the 4-apyH cation. On the other hand, for (4-apyH)ClO_4 such an explanation is not valid due to the value of the second moment observed being higher than that found for (4-apyH)$SbBr_4$. It seems that not all cations are able to perform the C_6' reorientations at room temperature. These cations are rigid and only reorientations of the NH_2 groups are allowed, taking into account the observed value of M_2. We should emphasize that the isotropic rotations of the cations have to be excluded over the room temperature phase, up to 300 K, since the observed value of M_2, being of the order of 2.6×10^{-8} T^2, is too large.

The experimental result for the proton spin–lattice relaxation times, T_1, is shown in figure 9(b). It should be noticed that the temperature dependence for T_1 does not show any minimum in the temperature region studied. Up to the phase transition at 243 K the relaxation function is single exponential. Above this phase transition, non-exponential recovery of ^1H magnetization has been observed. Such a recovery curve can be separated into two components, T_1^S and T_1^L ($T_1^S < T_1^L$), according to the equation

$$(M_0 - M_z(\tau))/M_0 = A_S \exp(\tau/T_1^S) + A_L \exp(\tau/T_1^L), \tag{3}$$

where M_0 and $M_z(\tau)$ are z-components of the magnetization at thermal equilibrium and at the time τ after the saturation sequence, respectively; A_S and A_L are constants ($A_S + A_L = 1$). In the whole temperature range studied the mutual relation between both observed components seems to be in a 1:4 ratio. At present, there is no satisfactory interpretation of this fact.

Unfortunately, the T_1 versus reciprocal temperature curve reveals no minima in the temperature range studied, so we were not able to determine the molecular dynamics parameters for the 4-apyH cations. From the slope of the T_1 versus temperature curve over the lowest-temperature phase (below 243 K), the activation energy was estimated to be 26 kJ mol^{-1}. This energy value may characterize the onset of the reorientation of the pyridinium ring, which diminishes the second-moment value insignificantly over the lowest-temperature phase. In turn, over the high-temperature phase (above 277 K), taking into account only the experimental points corresponding to the long component of T_1 (full points in figure 8(b)), E_a was found to be about 22.5 kJ mol^{-1}.

It should be underlined that the situation with M_2 and E_a characterizing the highest-temperature phase (above 277 K) of (4-apyH)ClO_4 resembles to some extent that found for (4-apyH)$SbBr_4$. By analogy to the interpretation of the NMR results for (4-apyH)$SbBr_4$ and other pyridinium salts, e.g. (pyH)SbX_4 [16], one can conclude that in the (4-apyH)ClO_4 crystal above 277 K the most probable mode of cation motion is the C_6'-type one. We should note that for in-plane 60° reorientational jumps of the cation about its C_6' axis, the theoretical value of M_2 equals 0.81×10^{-8} T^2, whereas the observed value amounts to about 2.6×10^{-8} T^2. In our opinion, one should expect the rotation of the ring between two sites instead of among six sites. Isotropic rotation of the $(4\text{-apyH})^+$ cations in the title crystal is excluded even at 300 K.

4. Discussion

On the basis of the x-ray and optical observations, the following sequence of the phase transitions is proposed:

	$P2_1$		C2		
		241 K		?	
Symmetry:	Monoclinic		Monoclinic		Trigonal
Phase:	Ferroelastic		Ferroelastic	Decomposition	Paraelastic

We should underline that the sequences of phase transitions are different during cooling and heating cycles. The discontinuous phase transition at 241/243 K (cooling/heating) is perfectly reversible, whereas the weakly first-order (or continuous) one at 277 K is observed only upon heating. At the present stage it is difficult to consider the nature and mechanism of the latter transition because it requires comparison of the crystal structures of the room temperature phases before and after cooling the crystal below the phase transition temperature at 241 K. Unfortunately we were not able to determine the crystal structure of the room temperature phase because of the distinct disorder of the cationic and anionic sublattices. The nature of this intermediate phase requires further investigation.

The postulated trigonal symmetry of the paraelastic phase may be suggested by numerous experimental results reported for closely related compounds [17, 18]. It was shown that many pyridinium salts crystallize in the trigonal system $R\bar{3}m$ or $R3m$, in which planar pyridinium rings are parallel to each other. This resembles the structural situation found in the title crystal.

A complex phase transition scenario was found for the similar ferroelectric compound, (pyH)ClO_4, which undergoes three phase transitions. These phase transitions are of the order–disorder type in which the dynamics of the cations and that of the anions change. In turn, numerous alkali perchlorates $MClO_4$ (M = Na, K, Rb, Cs) which undergo order–disorder phase transitions are characterized by both orientational disorder of ClO_4^- and a displacement of ions.

These data allow one to formulate a general conclusion that most of the phase transitions in such ionic salts are characterized by a complex mechanism in which all moieties are involved. In most of these cases we deal also with transitions either of the 'order–disorder' or of the 'displacive' type.

On the basis of the x-ray, ^{1}H NMR and dielectric response, the following change in the dynamics of molecules with temperature in the (4-apyH)ClO_4 crystal may be proposed. In the lowest-temperature phase, at 100 K, the structure is completely ordered. Approaching the 243 K phase transition from below, we can expect the releasing of some kind of motion of cations. From the ^{1}H NMR results we can only state that such a motion is characterized by a relatively large value of the activation energy (26 kJ mol^{-1}). Although the value of the real part of the electric permittivity is enhanced ($\sim$9 units) no dispersion is observed in the dielectric results. This means that the expected motion, which should be dielectrically active, has a relaxation time shorter than 10^{-9} s. The assumption that we deal exclusively with NH_2 group reorientations is in this case inappropriate. Such motion does not give a contribution to the T_1-value and is not dielectrically active. The most probable motion is a limited reorientation of the whole cation in the ring plane. Of course, this is related to some non-equivalent molecules. At the phase transition temperature (243 K) an enormous change in the crystal dynamics follows. It manifests itself as a drastic change in the dielectric increment ($\Delta\varepsilon \approx 14$ units), a rapid jump in the T_1-value and a quite large transition entropy value (17 J mol^{-1} K^{-1} = $R \ln 8$). It is obvious that in the mechanism of this phase transition we should consider the contribution of the 4-apyH cation and that of the ClO_4^- anions.

The NMR studies indicate neither in the high-temperature phase (III) nor—in particular—in the phase transition temperature, 243 K, releasing of the reorientation of C_6' type. Taking into account the smaller size and higher symmetry of the ClO_4^- anions compared with cations, one should expect a larger contribution of anions to the entropy change at the phase transition. Assuming a two-site model for the 4-apyH cations with a corresponding entropy effect of the order of $R \ln 2 = 5.76$ J mol^{-1} K^{-1}, a model with at least four sites should be assumed for the motion of the ClO_4^- moieties ($R \ln 4 = 11.52$ J mol^{-1} K^{-1}).

It might be interesting to compare the entropy change accompanying the phase transition in the title crystal with that observed in a salt containing the same cation, namely

(4-apyH)$SbBr_4$ [15]. The latter crystal is characterized by disorder of the 4-apyH cations and the rigid one-dimensional polymeric anion $(SbCl_4^-)_n$. It is obvious that the basic contribution to the entropy effect at $T_c = 224$ K, being of about 9.3 J mol^{-1} K^{-1}, is connected only with the dynamics of the 4-apyH cation. This might indicate that the dynamics of the perchlorate anions in the crystal presented contribute to the mechanism of the phase transition at 243 K, since the entropy change found is twice as large as that found for (4-apyH)$SbBr_4$.

Important information concerning the mechanism of the 243 K phase transition arises from the dielectric measurements. It is well known that, due to their symmetry and lack of dipole moment, the ClO_4^- anions cannot contribute to the dielectric increment ($\Delta\varepsilon$) at the phase transition point. There is no doubt that the reorientation of the organic cation has to lead to large changes in the dipole moment of the unit cell. By virtue of the size and the moment of inertia, the reorientation of the organic cations should be in turn significantly slower than that of the ClO_4^- groups. There is no doubt, therefore, that the observed dielectric relaxation process in the audio-frequency region ought to be assigned to the 4-apyH cation dynamics. The dielectric response around the phase transition at 243 K, however, seems to be complex. The distribution of the macroscopic relaxation times observed may be explained in terms of the dynamical inequivalence of (4-apyH) cations in the monoclinic $C2$ phase.

The appearance of the two components of the relaxation time T_1 above 243 K may be explained in terms of two independent (non-interacting) 4-apyH cations. This is in accordance with dielectric results, i.e. the presence of a distribution of relaxation times. The change of second moment, M_2, within the intermediate phase (243–277 K) may be interpreted as a gradual increase in freedom of rotational motion of the cation in the ring plane.

As was mentioned in the discussion of the NMR results, either the isotropic or the C_6' rotation of all cations is excluded above 277 K. Some cations may perform C_6' rotation, but for others only limited motions in the ring plane are allowed. There is no doubt that, upon heating, increase in the disorder of the ClO_4^- anions is expected.

5. Conclusions

(i) (4-apyH)ClO_4, revealed an interesting phase situation: a reversible first-order phase transition at 241/243 K (cooling/heating) and an irreversible weakly first-order (or continuous) one.
(ii) ^{1}H NMR and dielectric dispersion studies clearly proved that the 4-aminopyridinium cation dynamics contributed to the mechanism of the 241 K phase transition.
(iii) The order–disorder character of the transition at 241 K is clearly confirmed by a distinct transition entropy ($\Delta S \approx 17$ J mol^{-1} K^{-1}). The mechanism of this phase transition seems to be complex, because the dynamics of the cations and that of the anions are involved.
(iv) (4-apyH)ClO_4 revealed ferroelastic domain structure over the whole temperature range studied.

Acknowledgment

This work was supported partially by the Polish State Committee for Scientific Research (WM, project register 2 P03B 08822).

References

[1] Czarnecki P, Nawrocik W, Pająk Z and Wąsicki J 1994 *Phys. Rev.* B **49** 1511
[2] Czarnecki P, Nawrocik W, Pająk Z and Wąsicki J 1994 *J. Phys.: Condens. Matter* **6** 49

[3] Wąsicki J, Czarnecki P, Pająk Z, Nawrocik W and Szczepański W 1997 *J. Chem. Phys.* **107** 576
[4] Pająk Z, Czarnecki P, Wąsicki J and Nawrocik W 1998 *J. Chem. Phys.* **109** 6420
[5] Katrusiak A and Szafrański M 1999 *Phys. Rev. Lett.* **82** 576
[6] Teulon P, Delaplane R G, Olovsson I and Roziere J 1985 *Acta Crystallogr.* C **41** 479
[7] Roziere J, Williams J M, Grech E, Malarski Z and Sobczyk L 1980 *J. Chem. Phys.* **72** 6117
[8] Oxford Diffraction 2001 *CrysAlis 'CCD' and CrysAlis 'RED'* (Wrocław, Poland: Oxford Diffraction Sp. z o.o)
[9] Bruker AXS, Inc. 1999 *SHELXTL Software Package* Madison, WI 53711, USA
[10] Sheldrick G M 1997 *SHELXS97, Program for Solution of Crystal Structures* University of Göttingen
[11] Sheldrick G M 1997 *SHELXL97, Program for Crystal Structure Refinement* University of Göttingen
[12] Halvorson K E, Patterson C and Willett R D 1990 *Acta Crystallogr.* B **46** 508
[13] Jonscher A K 1983 *Dielectric Relaxation in Solids* (London: Chelsea Dielectric Press)
[14] van Vleck J H 1948 *Phys. Rev.* **74** 1168
[15] Hashimoto M, Hashimoto S, Terao H, Kuma M, Niki H and Ino H 2000 *Z. Naturf.* a **55** 167
[16] Okuda T, Aihara Y, Tanaka N, Yamada K and Ichiba S 1989 *J. Chem. Soc. Dalton Trans.* 631
[17] Czarnecki P, Wąsicki J, Pająk Z, Goc R, Małuszyńska H and Habryło S 1997 *J. Mol. Struct.* **404** 175
[18] Czarnecki P, Katrusiak A, Szafraniak I and Wąsicki J 1998 *Phys. Rev.* B **57** 3326